Langmuir

Article

pubs.acs.org/Langmuir

Effect of Cationic Polymers on Foam Rheological Properties

N. Politova,[†] S. Tcholakova,*[,†] K. Golemanov,[†] N. D. Denkov,[†] M. Vethamuthu,[‡] and K. P. Ananthapadmanabhan[‡]

[†]Department of Chemical Engineering, Faculty of Chemistry, Sofia University, 1 James Bourchier Avenue,1164 Sofia, Bulgaria

[‡]Unilever Global Research Center, Trumbull, Connecticut 06611, United States

Supporting Information

ABSTRACT: We study the effect of two cationic polymers, with trade names Jaguar C13s and Merquat 100, on the rheological properties of foams stabilized with a mixture of anionic and zwitterionic surfactants (sodium lauryloxyethylene sulfate and cocoamidopropyl betaine). A series of five cosurfactants are used to compare the effect of these polymers on foaming systems with high and low surface dilatational moduli. The experiments revealed that the addition of Jaguar to the foaming solutions leads to (1) a significant increase of the foam yield stress for all systems studied, (2) the presence of consecutive maximum and minimum in the stress vs shear rate rheological curve for foams stabilized by cosurfactants with a high surface modulus (these systems cannot be described by the Herschel−Bulkley model anymore), and (3) the presence of significant foam−wall yield stress for all foaming solutions. These effects are explained with the formation of polymer bridges between the neighboring bubbles in slowly sheared foams (for inside foam friction) and between the bubbles and the confining solid wall (for foam-wall friction). Upon addition of 150 mM NaCl, the effect of Jaguar disappears. The addition of Merquat does not noticeably affect any of the foam rheological properties studied. Optical observations of foam films, formed from all these systems, show a very good correlation between the polymer bridging of the foam film surfaces and the strong polymer effect on the foam rheological properties. The obtained results demonstrate that the bubble−bubble attraction can be used for efficient control of the foam yield stress and foam−wall yield stress, without significantly affecting the viscous friction in sheared foams.

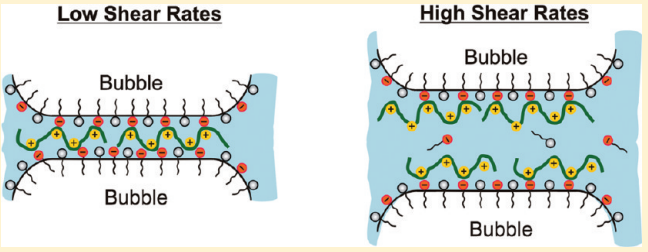

1. INTRODUCTION

During the past few decades, there has been a rapidly increasing interest in several scientific areas in the rheological behavior of foams.[1−12] In the course of the studies,[4−6] the researchers have formulated explanations and described quantitatively several of the basic dynamic properties of foams, such as their viscoelastic behavior,[4] yield transition,[5,11] viscous friction inside sheared foams,[9,10] and foam−wall friction.[7,8] It was shown that foam rheology is controlled by a subtle coupling of elastic and viscous effects: surface tension forces give rise to elastic mechanical response, caused by bubble deformation, whereas the viscous friction inside the foam films and/or surfactant adsorption layers leads to viscous dissipation of energy. The dependencies of foam elasticity, viscosity, and yield stress on the bubble size, surface tension, and solution viscosity were determined experimentally and explained theoretically. The respective scaling laws and theoretical models were used to describe a large variety of experimental data in terms of appropriate dimensionless quantities.

The performed studies demonstrated that, along with the general scaling of foam dynamic properties, the foams exhibit some strong system-specific effects.[7,8,10,12] These specific effects are related to the type of used foam stabilizers—surfactants, polymers, and/or particles. In a series of related experimental and theoretical studies, aimed to clarify the role of bubble surface mobility in foam rheology and some related phenomena, we observed and explained several significant effects of surfactant type on foam dynamics.[7−10,13−15] The experimental results demonstrated that two qualitatively different classes of surfactants could be distinguished:[15] The first class is represented by typical synthetic surfactants (sodium dodecyl sulfate (SDS), sodium lauryloxyethylene sulfate (SLES), and cocoamidopropyl betaine (CAPB)), which are characterized by a low surface dilatational modulus, E_D < 30 mN/m (LSM surfactants) and with fast relaxation of the surface tension after a rapid perturbation of the surface area (for less than 0.1 s). The second class of surfactants exhibits a high surface modulus, E_D > 100 mN/m (HSM surfactants) and relatively slow relaxation of the surface tension (for more than ca. 3 s). Typical surfactants from this class are the sodium and potassium salts of fatty acids (alkanecarboxylic acids), such as the lauric and myristic acids. With respect to foam rheology, the HSM surfactants lead to significantly higher viscous stress and different scaling laws of the shear stress vs shear rate (under otherwise equivalent conditions), as compared to the LSM

Received: September 11, 2011
Revised: December 11, 2011
Published: December 14, 2011

 © 2011 American Chemical Society dx.doi.org/10.1021/la2035517 | *Langmuir* 2012, 28, 1115−1126

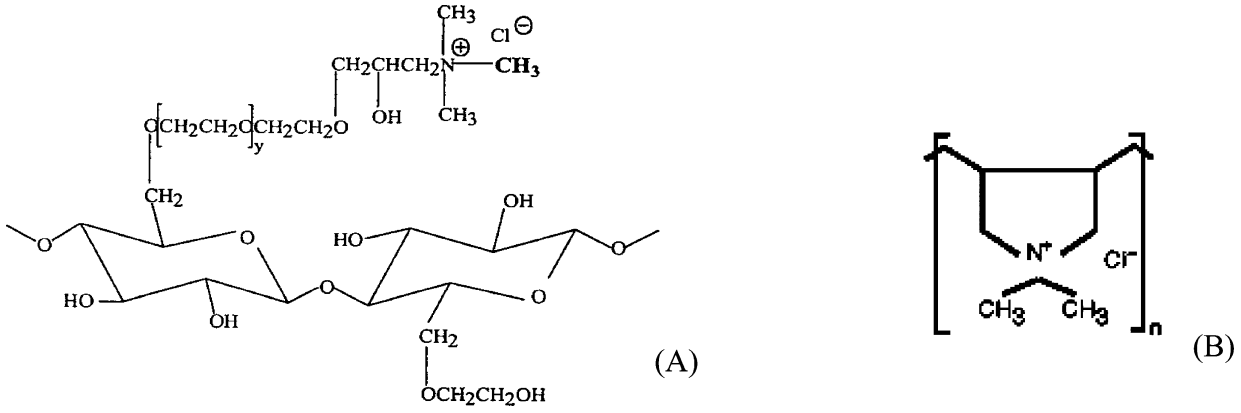

Figure 1. Chemical formulas of the studied polymers: (A) Jaguar C13s and (B) Merquat 100.

surfactants. Similar effects of the surfactant type were observed and discussed also by other research groups.[12,16−19]

The reasons for the observed differences between these two classes of surfactants were explained by theoretical models describing the viscous dissipation of energy in sheared foams:[9,10,15] (1) For the foam−wall friction, decisive is the different surface mobility of the bubbles − the surfaces of bubbles stabilized by LSM surfactants behave as tangentially mobile, whereas the surfaces of bubbles stabilized by HSM surfactants behave as tangentially immobile (rigid surfaces). The different surface mobilities result in different boundary conditions for the liquid flow in the wetting films, formed between the boundary foam bubbles and the confining solid wall, with a concomitant difference in the bubble−wall viscous stress. The scaling laws (m = 2/3 for mobile surfaces and m = 1/2 for immobile surfaces) emerge from the theoretical analysis of these two types of systems. (2) For the friction inside a sheared foam, the main difference comes from an additional contribution into the dissipated energy in the case of HSM surfactants; namely, the energy dissipation inside the adsorption layer of HSM surfactants is significant, due to the very high surface viscosity of the respective adsorption layers. In contrast, this contribution is negligible for the LSM surfactants, as compared to the viscous friction inside the foam films, formed between neighboring bubbles in flowing foam. The viscous friction in the films scales with the capillary number of power n = 1/2 (shown both experimentally and theoretically), whereas the surface dissipation scales with the shear rate (not with the capillary number) of power $n \approx 0.18$.

In many practical formulations, cationic polymers are added into the surfactant solutions. These cationic polymers are known to have a strong effect on the surfactant precipitation,[20] surface tension isotherms,[21] and thinning behavior of the respective foam films.[22−24] These observations suggest that the cationic polymers may have a strong impact on the foam rheological properties as well, without this effect being studied so far.

The major aim of the current study is to characterize experimentally the effect of two cationic polymers on the rheological properties of foams, stabilized with surfactants of low and high surface moduli. The polymers studied, with commercial names Jaguar C13s and Merquat 100, are widely used in shampoos, body wash formulations, cleaning liquids, and other home and personal care products. These polymers differ significantly in their chemical structure, charge density, and molecular weight.

We used the same basic surfactant system as in our previous studies[8,15]—a 2:1 mixture of SLES and CAPB. This system exhibits excellent foamability and foam stability and a low surface modulus of the bubbles. To modify the surface rheological properties of the foaming solutions, different cosurfactants were added to the SLES + CAPB solution. With respect to their effect on the rheological behavior of the foam, the chosen cosurfactants will be denoted as LSM and HSM surfactants. The additives from the LSM group possess a low surface modulus and do not have any significant effect on the foam rheological properties. In contrast, the cosurfactants from the HSM group lead to a much higher surface modulus of the bubbles, higher foam viscous stress, and stronger foam−wall friction. Therefore, the selected series of surfactant solutions covers a wide range of systems with different surface properties, which are typical for home and personal care applications.

Along with the rheological measurements (viscous friction inside the foam, foam−wall friction), we determined the viscosity and surface tension of the solutions used and the mean size of the bubbles in the foams. These are all quantities needed to interpret the foam rheological data.

The paper is organized as follows. The methods and materials are described in section 2. Section 3 explains how the foam rheological data are scaled. In section 4.1 we describe the properties of the studied solutions. In section 4.2 we present data for the mean bubble size in the formed foams. In sections 4.3 and 4.4 we describe the results for the effects of Merquat and Jaguar on the foam rheological properties. In section 4.5 we discuss the effect of polymers on foam film thinning and on equilibrium film thickness. These observations prove our explanation for the mechanism by which the polymers affect the rheological properties of the studied foams. The main conclusions are summarized in section 5.

2. MATERIALS AND METHODS

2.1. Materials. Two types of cationic polymers were studied, with commercial names Jaguar C13s (guar (hydroxypropyl)trimonium chloride, product of Rhodia) and Merquat 100 (poly-(diallyldimethylammonium chloride), product of Nalco); see Figure 1. According to the producer, the characteristics of Jaguar C13s are as follows: $M > 10^6$, charge density of 0.8 mequiv/g. The characteristics of Merquat 100 are $M = 1.5 \times 10^5$ Da and charge density of 6.2 mequiv/g.

The basic surfactant system is a mixture of the anionic surfactant SLES (product of STEPAN Co., with commercial name STEOL CS-170) and the zwitterionic surfactant CAPB (product of Goldschmith, with commercial name Tego Betaine F50). Five cosurfactes were

dx.doi.org/10.1021/la2035517 | Langmuir 2012, 28, 1115−1126

used—lauryl alcohol (LOH; product of Sigma), lauric acid (LAc; product of Arcos Organics), myristic acid (MAc; product of Fluka), Aminon L-02 bis(2-hydroxyethyl)lauramide (LADA; product of KAO), and cocoylmonoethanolamide (CMEA; product of the McIntyre Group). Cosurfactants were chosen in such a way that three of them (LAc, LOH, and MAc) ensure a high surface dilatational modulus (above 100 mN/m), whereas CMEA and LADA give a low surface modulus (below 10 mN/m).[8,15] Thus, we were able to compare three foaming solutions with a high surface modulus and three solutions with a low surface modulus.

The procedures for solution preparation were as follows: First, we prepared a stock solution of SLES + CAPB (called for brevity "basic surfactants" and abbreviated as "BS"). The weight ratio of the active SLES and CAPB in the studied BS mixtures was fixed at 2:1, and the total surfactant concentration was C_{TOT} = 10 wt %.

Mixtures of BS + cosurfactant were prepared by dissolving 0.5 wt % cosurfactant in the concentrated BS solution under mild stirring and heating (if needed) until a clear solution was formed. The solution was heated at 60 °C for MAc and at 45 °C for LAc and LOH, while CMEA and LADA were dissolved at room temperature. For the foaming experiments, these solutions were diluted 20-fold with deionized water.

Stock solutions of Merquat of the desired concentration (up to 0.2 wt %) were prepared by dissolving the required amount of Merquat in water at room temperature. These solutions were clear during storage (which was no longer than 5 days) before their use for preparation of mixed surfactant−polymer solutions for foam experiments.

Stock solutions of Jaguar with the desired concentration (up to 0.1 wt %) were prepared by applying vigorous stirring on a magnetic stirrer and heating to 40 °C. The stirring was continued for at least 30 min until a clear solution was obtained. After being cooled to room temperature, the obtained solutions became opalescent. To remove the insoluble residues, we applied centrifugation of these solutions at 5000 rpm for 30 min.

Diluted solutions of BS + cosurfactant + polymer were prepared in the following way: A solution with a concentration 2 times higher than the necessary final concentration of the polymer was prepared, which was afterward mixed in a 1:1 ratio with the 10-fold diluted BS−cosurfactant mixed solution. Therefore, the final Merquat solutions contained 0.5 wt % SLES+CAPB (at a 2:1 ratio) + 0.025 wt % cosurfactant + 0.025, 0.05, or 0.1 wt % Merquat. Because Jaguar is less soluble than Merquat, the Jaguar concentration in the final solution was 0.01, 0.02, or 0.04 wt %. In some of the Jaguar-containing systems, we used a 150 mM NaCl solution for dilution, instead of pure water. The presence of NaCl led to formation of precipitates, if working with a polymer concentration of 0.02 wt % and higher. Therefore, the concentration of Jaguar in the final solution containing 150 mM NaCl was kept low, 0.01 wt % polymer.

2.2. Characterization of the Foaming solutions. All experiments discussed in the paper are performed at $T = 20 \pm 0.3$ °C.

The viscosity of the surfactant solutions, μ, was measured with a thermostated capillary viscometer after calibration with pure water. The surface tension of these solutions, σ, was measured with the Wilhelmy plate method on a K100 tensiometer (Krüss GmbH, Germany). The surface dilatational modulus was measured at 0.2 Hz frequency and 0.5% amplitude of drop area oscillations on a DSA 100 instrument, equipped with an oscillating drop module (ODM)/expanding drop module (EDM) (Krüss GmbH, Germany).

2.3. Foam Generation and Characterization. To generate foam with air volume fraction $\Phi \approx 0.9$, we used the following procedure: First, 1 mL of surfactant solution was sucked into a 20 mL syringe, equipped with a stainless steel needle with an internal diameter of 2.5 mm (Hamilton, catalog no. 7730-05). Then 9 mL of air was captured in the syringe, forming a coarse foam with large bubbles. These large bubbles were broken into much smaller bubbles by using a series of ejection/injection cycles of the foam through the needle. In this way, foam containing bubbles of submillimeter diameter was produced.

The air volume fraction in the formed foams was determined gravimetrically. A syringe with known volume (20 mL) was filled with foam and weighed. The air volume fraction in the foam is determined from the relation $\Phi = 1 - m_F/(V_F\rho)$, where m_F is the mass of the foam in the syringe, V_F is the respective foam volume, and ρ is the mass density of the foaming solution.

The bubble size distribution in the formed foams was determined by using the procedure of Garrett et al.[25,26] The foam was spread in a small Petri dish, and an optical triangular prism was placed on top of the dish, in direct contact with the foam. The foam is illuminated by diffuse white light through one of the prism sidewalls, whereas the foam observation is made through the other sidewall of the prism by a video camera. The bubbles contacting the prism wall are thus visualized, and the projected area of each bubble on the wall surface can be measured. The bubble images were processed via the shareware computer program ImageJ, released by the National Institutes of Health (NIH), and the bubble size distribution was determined by using the relation $R_B = (A_{BP}/\pi)^{1/2}$, where A_{BP} is the projected area of a given bubble in contact with the prism wall. For scaling of the rheological data, the mean surface-to-volume radius, R_{32}, was used:

$$R_{32} = \sum_i R_i^3 / \sum_i R_i^2 \quad (1)$$

where the sums are taken over all measured bubbles in a given sample.

The rheological properties of the studied foams were determined via parallel plate rheometry with a Gemini rotational rheometer (Malvern Instuments, U.K.) at a temperature of 20 °C. Two types of experiments were performed.

2.3.1. Friction inside a Sheared Foam (Figure S1A in the Supporting Information). In these experiments, sandpaper (P100) was glued on both plates of the rheometer to suppress foam−wall slip. During the experiment, the shear rate, $\dot{\gamma}$, is varied logarithmically from 0.02 to 200 s^{-1} and the shear stress is recorded, $\tau = \tau(\dot{\gamma})$. Control experiments showed that the same results are obtained if the foam is sheared in discrete steps of the shear rate, as in our previous studies.[7] In these experiments, the shear stress is higher than the yield stress of the foam, $\tau > \tau_0$, and the total stress measured by the rheometer includes viscous dissipation in the bulk of the foam (bubble−bubble friction).

2.3.2. Foam−Wall Friction (Figure S1B in the Supporting Information). In these experiments, sandpaper (P100) was glued only on the lower plate, whereas a smooth glass plate was glued on the upper (rotating) plate. In this way, there was no slip between the foam and the lower plate, whereas the foam slipped over the upper plate. During the experiment, the shear rate is varied and the shear stress is kept below the yield stress of the foam, $\tau < \tau_0$, to prevent shear flow in the bulk foam. In this case, the measured shear stress is due entirely to the viscous friction between the foam and the smooth wall.

All experiments were performed by using parallel plates with a radius of 20 mm and the gap width between the upper and the lower plates fixed at 3 mm. Control experiments at smaller gaps (2.5, 2, and 1.5 mm) showed no dependence of the results on the used gap for any of the systems studied; see Figure S2 in the Supporting Information as an illustration. This independence of the rheological results on the gap width indicates no significant effects of the wall-slip or shear bending.

2.4. Observation of Foam Films in a Capillary Cell. Foam films of submillimeter size were formed and observed in a capillary cell to obtain information for the film-thinning behavior and the equilibrium film thickness. The observations were made by using the method of Scheludko.[27] The films were formed from a biconcave drop, placed in a short capillary (i.d. 2.5 mm, height 3 mm), by sucking out liquid through a side orifice. The observations were performed in reflected monochromatic light by means of an Axioplan microscope (Zeiss, Germany), equipped with a long-distance objective, Zeiss Epiplan 20×/0.40, charge-coupled device (CCD) camera, video recorder, and monitor. Depending on the film thickness, the light reflected by the film has different colors. From the color and from the intensity of the light reflected from the foam film, one can determine the film thickness with rather good precision.[27] The films that are thicker than 100 nm appear colored. The films with a thickness of about 100 nm appear white (bright), those with a thickness of about 50 nm appear gray, and those with a thickness under 30 nm appear dark.

dx.doi.org/10.1021/la2035517 | Langmuir 2012, 28, 1115−1126

3. THEORETICAL BACKGROUND

3.1. Friction inside a Sheared Foam. The dependence of the total stress on the rate of strain for a steadily sheared foam is described well by the Herschel−Bulkley model, which includes three parameters—yield stress, τ_0, consistency, k, and power-law index, n:

$$\tau = \tau_0 + \tau_V(\dot{\gamma}) = \tau_0 + k\dot{\gamma}^n \quad (2)$$

Here $\dot{\gamma}$ is the applied shear rate, τ is the total shear stress, and τ_V is the viscous stress. As discussed in the literature,[1−7] it is appropriate to scale the yield stress and viscous stress by the bubble capillary pressure, $P_C \approx \sigma/R_{32}$, whereas the dimensionless shear rate is adequately represented by the so-called "capillary number", Ca:

$$\tilde{\tau}_0 = \frac{\tau_0}{\sigma/R_{32}}; \quad \tilde{\tau}_V = \frac{\tau_V}{\sigma/R_{32}}; \quad \mathrm{Ca} = \frac{\mu\dot{\gamma}R_{32}}{\sigma} \quad (3)$$

Here $\tilde{\tau}_0$ is the dimensionless yield stress, $\tilde{\tau}_V$ is the dimensionless viscous stress, and R_{32} is the mean volume surface radius, while σ is the surface tension and μ is the viscosity of the foaming solution.

It is shown in the literature[1,5,6,28] that the dimensionless yield stress is a function of the volume fraction of the dispersed phase, Φ, and of the bubble polydispersity. Princen[1,5] found experimentally the following empirical expression for $\tilde{\tau}_0$:

$$\tilde{\tau}_0 = \Phi^{1/3}(-0.080 - 0.114\log(1-\Phi)) \quad \text{at} \quad \Phi > 0.8 \quad (4)$$

The above equation is applicable for typical polydisperse foams and emulsions. For monodisperse systems, Mason et al.[28,29] found the following equation to describe better his experimental data:

$$\tilde{\tau}_0 = 0.51(\Phi - 0.62)^2 \quad (5)$$

For dispersions with $\Phi = 0.9$, like those used in our study, the Princen equation predicts $\tilde{\tau}_0 = 0.033$, whereas the Mason equation predicts $\tilde{\tau}_0 = 0.040$.

In our previous studies,[9,10] we developed a theoretical model which accounts for the dissipated energy inside the foam films and on the bubble surface.[9,10] At negligible surface dissipation (low surface modulus of the foaming solution), we derived[9,10] the following expression, which accounts for the viscous dissipation inside the foam films, formed between the sliding bubbles in a sheared foam at $\Phi > 0.74$:

$$\tilde{\tau}_{VF} \approx 1.2\Phi^{5/6}\frac{(\Phi - 0.74)^{0.1}}{(1-\Phi)^{0.5}}(\mathrm{Ca}^{0.47}) \quad (6)$$

For foams with a low surface modulus, at $\Phi = 0.9$, this model predicts $\tilde{\tau}_V = 2.89(\mathrm{Ca}^{0.47})$. The contribution of the surface dissipation of energy to the total viscous stress (at high surface modulus of the foaming solution) is described by the expression[10]

$$\tilde{\tau}_{VS} \approx 9.8\pi\Phi\frac{E_{LS}}{\sigma}{a_0}^2 \quad (7)$$

where E_{LS} is the surface loss modulus and a_0 is the relative amplitude of the changes of the bubble surface area in the flowing foam (as a result of collisions with the neighboring bubbles). The comparison between this theoretical expression and the experimental data showed that the viscous stress created by the surface dissipation of energy on the bubble surface is proportional to the shear rate with a power law index of around 0.18:[10]

$$\tilde{\tau}_{VS} \approx A\Phi\dot{\gamma}^{0.18} \quad (8)$$

The multiplier A in eq 8 accounts for the role of the surface viscous modulus and is sufficiently large to make this contribution significant only for specific surfactants or cosurfactants (such as fatty acids and lauryl alcohol) with a high surface modulus.

We should mention briefly here that the structural mechanisms, explaining the rate dependence of the foam shear stress, are still under debate in the literature.[30,31] For example, on the basis of 3D simulations of sheared dispersions of elastic spheres (modeling suspensions of gel particles and emulsions), Seth et al.[30] came to the conclusion that the elastic stress in such dispersions is strongly dependent on the shear rate. In contrast, Sexton et al.[31] found in 2D simulations of sheared foams only a weak variation of the elastic stress with the strain rate. Although these different scenarios might lead to somewhat different interpretations of the shapes of the shear stress vs shear rate curves, none of the main conclusions of the current study, related to the effect of polymers on the yield stress (defined as the stress limit at low shear rates), would be changed when accepting one or another mechanistic explanation. We have chosen our model[9,10] to discuss the experimental data, mainly because this is the only model which suggests an explicit expression for the thickness of the dynamic foam films, formed between the colliding bubbles in sheared foams; this film thickness can be compared to the size of the adsorbed polymer molecules (see eq 12 below and the discussion below it). The expression for the film thickness proposed in ref 30 is based on assumptions which are rather questionable (the film thickness is taken from the particle−wall friction and applied without additional argumentation to the particle−particle friction).

3.2. Foam−Wall Friction. The dimensional wall stress, due to foam−wall friction, can usually be fitted by one of the following equations:

$$\tau_W = k_W{V_W}^m \quad (9)$$

$$\tau_{TW} = \tau_{0W} + k_W{V_W}^m \quad (10)$$

Here τ_{TW} is the total wall stress, τ_W is the viscous wall stress, V_W is the velocity of the foam relative to the solid wall, and m is the power-law index for the foam−wall friction. Equation 10 assumes that there is a yield stress for the foam−wall relative motion, τ_{0W}, which must be overcome for foam sliding to occur (with respect to the solid wall). Equation 9 does not contain such a term, and the only stress is the viscous one, due to friction between the boundary layer of bubbles in the foam and the confining solid wall.

For scaling of the results for foam−wall friction, the dimensionless velocity of the foam is used:

$$\tilde{V}_W = \mu V_W/\sigma \quad (11)$$

The dimensionless velocity is equivalent to the capillary number, defined for the experiments of friction inside a sheared foam. The power-law index for foam−wall friction takes a value of $m \approx 1/2$ for a tangentially immobile (rigid) bubble surface[7,8] and $m \approx 2/3$ for bubbles with tangential mobility.[7]

dx.doi.org/10.1021/la2035517 | Langmuir 2012, 28, 1115−1126

These dimensionless quantities are used in the following consideration of the various systems, because they allow one to reveal the nontrivial effects related to the specific surface properties of the systems.

4. RESULTS AND DISCUSSION

4.1. Solution Properties. *4.1.1. Precipitation Boundary.* This series of experiments is aimed at determining the precipitation boundary of solutions containing 0.5 wt % BS (SLES + CAPB, 2:1) ± 0.025 wt % cosurfactant when adding polymer. The concentration of Merquat was varied up to 0.1 wt %. All solutions were clear at 0.025 wt %, slightly turbid at 0.05 wt %, and very turbid at 0.1 wt % Merquat, but no large particles were seen to segregate (no clear phase separation was observed). The solutions of 0.2 wt % Merquat contained sediments of surfactant−polymer aggregates, and no further experiments were performed with these latter solutions.

The concentration of Jaguar was varied up to 0.04 wt %. All solutions, prepared with deionized water, were clear at 0.01 wt %, slightly turbid at 0.02 wt %, and very turbid at 0.04 wt % Jaguar, where some particles were seen but remained dispersed in the solution. At higher Jaguar concentrations, a large amount of precipitates were formed and no further experiments were performed with these latter solutions.

The presence of 150 mM NaCl in the Jaguar-containing systems led to formation of jelly-like sediments for all solutions with 0.02 wt % Jaguar. For this reason, the experiments with systems containing 150 mM NaCl were performed at a polymer concentration of 0.01 wt % only, where the solutions were slightly opalescent and no sediment was formed.

4.1.2. Surface Tension and Surface Dilatational Modulus of the Solutions Studied. The experimental data for the surface tension and the surface modulus of the studied foaming solutions are summarized in Table 1. Briefly, these results can be summarized as follows.

Table 1. Surface Tension and Total Surface Dilatational Modulus, E_D, for 0.5 wt % BS and 0.5 wt % BS + 0.025 wt % Cosurfactant Solutions without Added Polymer in the Presence of 0.1 wt % Merquat or in the Presence of 0.02 wt % Jaguar[a]

	surface tension, σ, mN/m			surface modulus, E_D, mN/m		
surfactant system	no polymer	+ 0.1 wt % Merquat	+ 0.02 wt % Jaguar	no polymer	+ 0.1 wt % Merquat	+ 0.02 wt % Jaguar
BS	28.8	29.0	29.1	4.2	4.0	4.5
BS + CMEA	28.3		28.7	3.5		
BS + LADA	28.0		29.1	3.7		
BS + LAc	26.2		26.3	170		
BS + MAc	22.6	22.6	22.6	400	280	400
BS + LOH	21.0		21.9	250		

[a]The surface dilatational modulus is measured by the oscillating drop method at a frequency of 0.2 Hz and 0.5% area deformation at 20 °C.

The surface tension measurements showed that 0.5 wt % BS has σ = 28.8 ± 0.2 mN/m. The addition of 0.025 wt % cosurfactant CMEA decreases σ to 28.3 mN/m, and that of LADA decreases σ to 28.0 mN/m. Solutions containing cosurfactants with a high surface modulus have lower surface tensions: 26.2 mN/m for LAc-containing, 22.6 mN/m for MAc-containing, and 21.0 mN/m for LOH-containing solutions.

The addition of Merquat at concentrations of 0.025, 0.05, and 0.1 wt % to the BS and BS + MAc solutions does not significantly affect the surface tension; it was the same in the frame of experimental accuracy.

When Jaguar was added, the surface tension of all studied solutions of the BS + LSM cosurfactant type was $\sigma \approx 29 \pm 0.2$ mN/m. It seems that the addition of Jaguar to these solutions slightly increases σ, which could be due to adsorption of some of the surfactant molecules on the dissolved polymer chains (the effect is small, however). For the BS + HSM cosurfactant solutions, no detectable effect of Jaguar on the equilibrium surface tension was found.

Therefore, at these concentrations of surfactants (well above the critical micelle concentration (cmc)) and polymers, Merquat and Jaguar have no strong effect on the equilibrium surface tension of the solutions studied.

The surface dilatational modulus of BS, BS + CMEA, and BS + LADA solutions was measured to be relatively low, $E_D \approx 4 \pm 0.5$ mN/m. No significant effect of Merquat and Jaguar on E_D was detected for these systems. However, a noticeable effect of Merquat on E_D was found for BS + MAc solutions: E_D decreased from 400 to 280 mN/m after the addition of Merquat. Still, the surface modulus of BS + MAc + Merquat systems remains much higher than the surface modulus of BS and BS + Merquat solutions; see Table 1. No noticeable effect of Jaguar was determined on the surface rheological properties of BS and BS + MAc solutions. Therefore, the surface modulus of all studied solutions is controlled by the used cosurfactant.

4.1.3. Solution Viscosity. The viscosity of the polymer-containing foaming solutions was slightly higher than that of water, between 1.05 and 1.1 mPa·s. The viscosity of the polymer-free solutions was practically equal to that of water, 1.0 ± 0.02 mPa·s.

4.2. Mean Bubble Size in the Foams. One important characteristic of the studied foams is the mean volume surface radius of the bubbles, R_{32}, which is used for scaling of the rheological data; see section 3. Experimental results for R_{32}, for the foams formed from BS + Merquat, BS + MAc + Merquat, BS + Jaguar, and BS + MAc + Jaguar solutions, are presented in Figure S3 in the Supporting Information. One sees that the bubbles in the foams stabilized by BS are bigger than those stabilized by BS + MAc. This experimental fact is explained by the higher friction between the bubbles in the systems containing cosurfactants with HSM; see the systematic study of this effect in ref 14.

The addition of Jaguar to solutions of the BS + LSM cosurfactant type leads to some decrease of the mean bubble radius, but this effect is relatively small. For the systems of the BS + HSM cosurfactant type, the effect of Jaguar on R_{32} is scattered: in some of the foams we observe slightly smaller bubbles in the presence of Jaguar (e.g., with MAc as the cosurfactant), whereas for other systems larger bubbles are observed (e.g., with LAc, data not shown).

The addition of Merquat to BS and BS + MAc solutions leads to formation of larger bubbles for both surfactant systems. The size of the bubbles increases with increasing Merquat concentration. The effect is not large, but seems real. Probably, it reflects the interaction between Merquat and surfactants in the bulk solution, which decreases the rate of surfactant adsorption during foaming.

dx.doi.org/10.1021/la2035517 | Langmuir 2012, 28, 1115−1126

4.3. Friction inside the Foam. The results for the dimensionless viscous stress, as a function of the capillary number, for foams stabilized by mixtures of SLES + CAPB (BS) and SLES + CAPB + MAc (BS + MAc) at different Merquat concentrations are presented in Figure 2. One sees that the addition of Merquat to these systems does not affect the rheological properties of the foams studied. The dimensionless viscous stress, as a function of the capillary number, merges around a master line with a power-law index $n \approx 0.25$ for all systems containing MAc and $n \approx 0.47$ for all systems without MAc; see Figure 2.

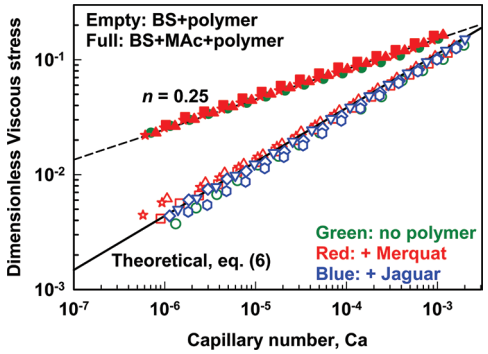

Figure 2. Dimensionless viscous stress as a function of the capillary number for friction inside foams stabilized by BS (red empty circles), BS + MAc (red full circles), BS + 0.025 wt % Merquat (red empty triangles), BS + 0.05 wt % Merquat (red empty squares), BS + 0.1 wt % Merquat (red empty stars), BS + 0.01 wt % Jaguar (blue empty triangles), BS + 0.02 wt % Jaguar (blue empty tilted squares), BS + 0.04 wt % Jaguar (blue empty hexagons), BS + MAc + 0.025 wt % Merquat (red full triangles), BS + MAc + 0.05 wt % Merquat (red full squares), and BS + MAc + 0.1 wt % Merquat (red full stars). The solid line is drawn according to eq 6. The dashed line has a slope of 0.25.

The results for the foams formed in BS + Jaguar solutions are also shown in Figure 2. Again, the experimental data merge around a master line with $n = 0.47$, and no significant effect of Jaguar on the viscous friction is detected (the results for the BS + MAc solutions are not shown for reasons explained below). The comparison between the experimental data for the dimensionless viscous stress and the theoretical expressions (see eqs 6 and 7) shows that the main contribution to the friction in the foams, stabilized by BS + Merquat and BS + Jaguar, is the friction in the foam films between the neighboring sliding bubbles, whereas for the BS + MAc + Merquat systems it is the energy dissipated in the adsorption layer.

Another important characteristic of the rheological behavior of the foams is their yield stress. As seen from Figure 3A, Jaguar is able to significantly increase the yield stress of the foams formed in BS + Jaguar solutions. The dimensionless yield stress of the polymer-containing foams is presented in Figure 3B; one sees that the dimensionless yield stress increases significantly with an increase of the Jaguar concentration. In contrast, Merquat has no effect on the dimensionless yield stress; its values are close to those measured by Princen[1] with polydisperse emulsions at the same volume fraction of the dispersed phase, $\Phi \approx 0.9$.

Therefore, the first significant effect of Jaguar is to increase the foam yield stress in BS + Jaguar systems. As we show in section 4.5, this effect is due to bridging of the surfaces of neighboring bubbles by polymer molecules. The second very significant effect of Jaguar is observed for foams formed in BS +

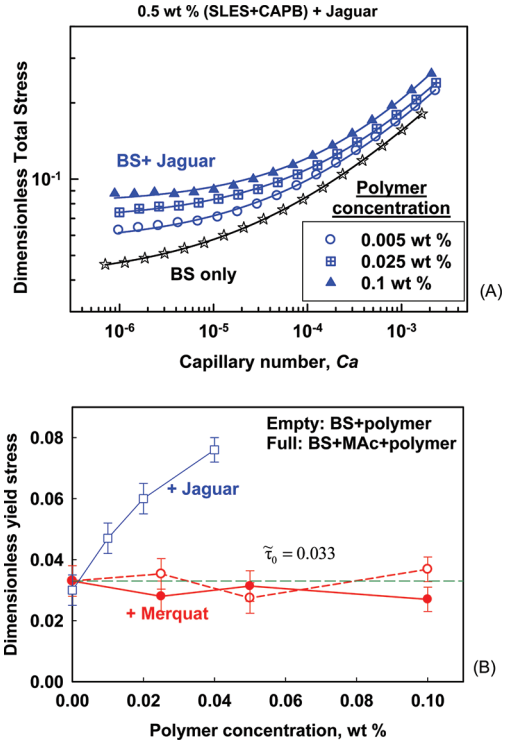

Figure 3. (A) Dimensionless total stress as a function of the capillary number for foams formed in BS + Jaguar solutions. The data for 0.5 wt % BS are represented by black stars, empty circles represent data obtained in the presence of 0.005 wt % polymer, crossed squares represent data obtained in the presence of 0.025 wt % polymer, and full triangles represent data obtained in the presence of 0.1 wt % polymer. The curves represent the best fits of the experimental data according to the Herschel–Bulkley equation. The air volume fraction is 0.9 for all foams. (B) Dimensionless yield stress as a function of the polymer concentration for foams stabilized by SLES + CAPB + Merquat (empty red circles), SLES + CAPB + MAc + Merquat (full red circles), and SLES + CAPB + Jaguar (empty blue squares). The green line represents the dimensionless yield stress of 0.033, which is predicted by eq 4.

HSM cosurfactant solutions; see Figure 4. For BS + MAc + Jaguar foams, Figure 4A, the total stress at a given Ca increases with an increase of the Jaguar concentration. Moreover, the shape of the τ vs Ca curve cannot be fitted by the Herschel–Bulkley law for these systems, because the shear stress passes through a maximum as Ca is increased. Above a certain threshold Ca, which is around 2×10^{-5}, the stress starts to increase again and approaches the rheological curve for the polymer-free systems.

To further analyze the effect of Jaguar on the foam rheological properties, we performed additional experiments with systems stabilized with mixtures of BS + cosurfactant in the presence of 0.02 wt % Jaguar. As LSM cosurfactants we used CMEA and LADA, whereas as HSM cosurfactants we used LAc and LOH. The obtained results can be summarized as follows:

(1) For all foams stabilized by BS + LSM cosurfactant, in the presence of Jaguar, we found that the data for the total stress vs shear rate can be described by the Herschel–Bulkley law, eq 2. From the best interpolation fit, we determined the dimensionless yield stress to be $\tilde{\tau}_0 = 0.06$ for both CMEA- and LADA-containing solutions. Note that this value coincides with the value determined for

dx.doi.org/10.1021/la2035517 | Langmuir 2012, 28, 1115–1126

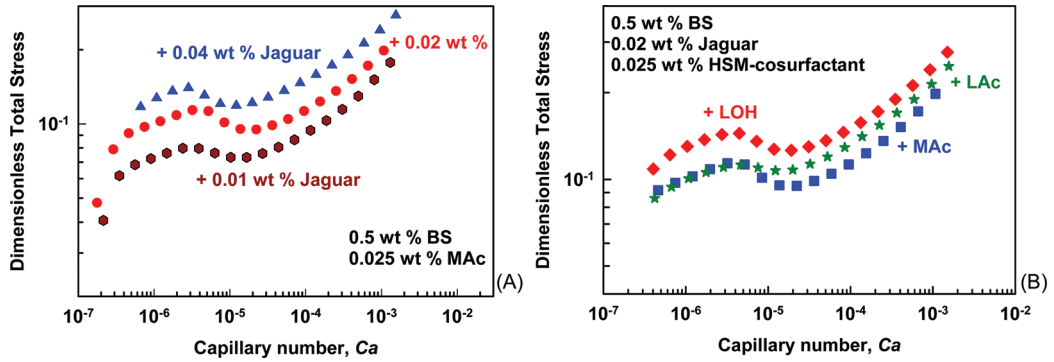

Figure 4. Dimensionless total stress as a function of the capillary number, Ca, for foams stabilized by (A) BS + MAc + Jaguar solutions with different concentrations of Jaguar as indicated in the figure and (B) BS + Jaguar + different cosurfactants as indicated in the figure.

BS–Jaguar foams at 0.02 wt % Jaguar (Figure 3B). Therefore, we can conclude that the addition of 0.02 wt % Jaguar to BS–LSM cosurfactant solutions increases the dimensionless yield stress approximately 2-fold compared to that of Jaguar-free systems. No significant effect of Jaguar on the dependence of the viscous stress on the capillary number was seen for these systems. Thus, for the systems stabilized by BS + LSM cosurfactant, the main effect of Jaguar is to increase the dimensionless yield stress without affecting the viscous friction.

(2) The experimental data for the BS + HSM cosurfactant systems, in the presence of Jaguar, could not be described by the Herschel–Bulkley law, which predicts a monotonic increase of the stress with increasing shear rate. In contrast with this prediction, we see that the stress passes initially through a maximum at Ca $\approx 5 \times 10^{-6}$, followed by a minimum at Ca $\approx 2 \times 10^{-5}$ and a monotonic increase of $\tilde{\tau}$ with a further increase of Ca; see Figure 4B. The maximum in the stress value is $\tilde{\tau} \approx 0.14$ for LOH-containing foams and $\tilde{\tau} \approx 0.11$ for LAc- and MAc-containing foams, which is 3–4 times larger than the predictions of Princen's and Mason's formulas. It should be mentioned that the maximum values of the stress varied from experiment to experiment (viz., they were not very reproducible), but the shape of the curve was very robust.

The observed maximum in the total shear stress vs capillary number curves can be explained in the following way. The polymer chains can form bridges between the neighboring bubbles in still foam. These bridges act as elastic springs, which make the foam behave as an elastic medium at small strains. At a given critical shear stress, these bridges start to break and the shear stress decreases. After the polymer "bridges" are broken, the shear stress increases further with the shear rate, due to the increasing viscous friction between the bubbles at higher shear rates; see Figure 5. The observed decrease of foam shear stress in the limit of small Ca is explained by the fact that the polymer adsorption is physical in these systems (no covalent bonds are formed), which allows the polymer molecules to rearrange with time and thus relax the elastic stress when the shear rate is very low.

Such polymer bridges also explain the higher dimensionless yield stress for BS + LSM cosurfactant systems containing Jaguar. However, for these systems the transition from bridged to separated bubbles is much smoother, and hence, the

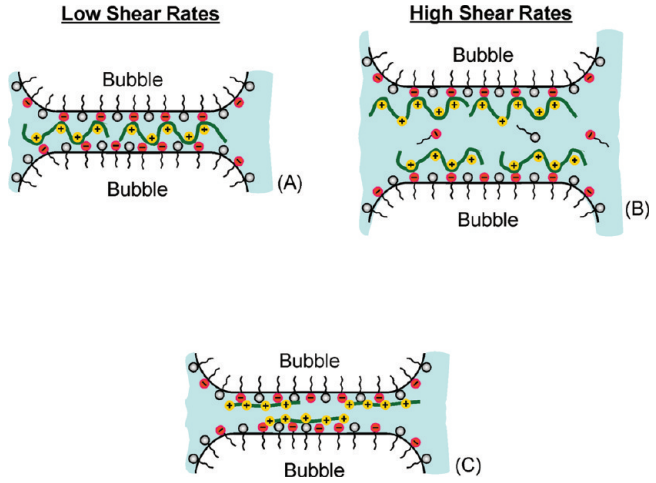

Figure 5. Schematic presentation of the foam film between two neighboring bubbles. (A) The film surfaces are bridged by cationic polymer chains in foams at rest or subjected to slow shear deformation. (B) At high shear rates, the film thickness is larger than the size of the adsorbed polymer molecules and the polymer bridges are broken. (C) For highly charged linear cationic polymers, the polymer molecules may lie close to the solution surface, without bridging the foam film surfaces even for equilibrium films in an immobile foam. The obtained results show that configuration A is typical for Jaguar C13s whereas configuration C is realized for Merquat 100.

rheological curves are fitted well by the Hershel–Burkley equation.

The mechanistic explanation for the different effects of Jaguar on the rheological behavior of foams, with high and low surface moduli of the foaming solutions, is still obscured. In our previous studies we found that there is a condensed surfactant phase on the surface of the bubbles, stabilized with the mixture BS + fatty acid.[8] This condensed phase is mostly composed of fatty acid molecules which provide rigidity and a high surface modulus of the respective foaming solution. The peculiar rheological behavior of the foams containing Jaguar and such HSM cosurfactants should be related to the anchoring of the polymer molecules to the rigid surface phase. The rigidity of the adsorption layer in these systems probably leads to the formation of a strong network of polymer bridges between the bubble surfaces, which is difficult for rearrangement and breakage. In contrast, there is no surface condensed phase in the systems with LSM cosurfactants, so that the network of polymer bridges (if formed) can rearrange through a lateral

dx.doi.org/10.1021/la2035517 | Langmuir 2012, 28, 1115–1126

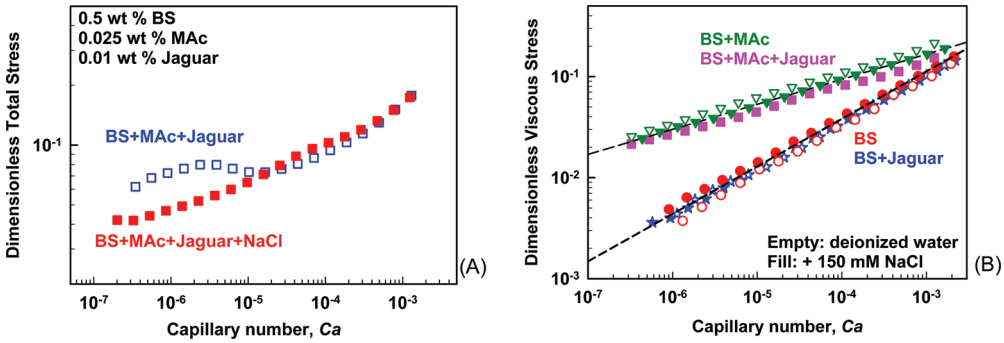

Figure 6. (A) Dimensionless total stress as a function of the capillary number, Ca, for foams stabilized by BS + MAc + Jaguar (empty blue squares) and BS + MAc + Jaguar + 150 mM NaCl (full red squares). (B) Dimensionless viscous stress as a function of the capillary number for BS (red circles), BS + Jaguar (blue stars), BS + MAc (green triangles), and BS + MAc + Jaguar (pink squares) without NaCl (empty symbols) and with 150 mM NaCl (full symbols). The concentration of BS is 0.5 wt %, that of MAc is 0.025 wt %, and that of Jaguar is 0.01 wt %.

motion of the adsorbed surfactant molecules, thus making this network weaker.

From the experimental data presented in Figures 2 and 4, we can conclude that there is a transitional capillary number above which the presence of Jaguar in BS + HSM cosurfactant solutions does not affect the bubble sliding in the sheared foams. This transitional capillary number is most probably related to the thickness of the dynamic foam films, which are formed between the bubbles in a sheared foam. The film thickness increases with the foam shear rate and could be significantly larger than the equilibrium thickness of the foam films in the still foam. One could expect that the polymer molecules will not strongly affect the foam flow when the thickness of the dynamic films is larger than the dimensions of the adsorbed polymer molecules. In other words, the polymer molecules can bridge the film surfaces when the film thickness is sufficiently small.

We estimated theoretically the thickness of the dynamic foam films in a sheared foam to compare this thickness to the size of the adsorbed polymer molecules (section 4.5). The model developed in our previous studies[9,10] was used to estimate the thickness of the dynamic films in a steadily sheared foam:[10]

$$h_1 \approx bR_0(\mathrm{Ca}^{1/2}) \tag{12}$$

where R_0 is the mean bubble radius, Ca is the capillary number, and b is between 0.15 and 0.25 for foams with $\Phi = 0.9$. The experimental results presented in Figures 2 and 4 show that the capillary number below which the friction between the bubbles is significantly affected by the presence of Jaguar is Ca $\approx 1 \times 10^{-6}$ for foams stabilized by BS + LSM cosurfactant and Ca $\approx 5 \times 10^{-6}$ (the maximum in the rheological curve) for BS + HSM cosurfactant foams. Note that the mean bubble size in LSM cosurfactant foams is $R_{32} \approx 240$ μm, whereas in HSM cosurfactant foams it is $R_{32} \approx 130$ μm. Using these values, we estimate that the film thickness at which the bubbles are significantly affected by the presence of Jaguar is $h_1 \approx 70$ nm for both types of solutions—containing LSM and HSM cosurfactants. As we will see in section 4.5, the optical observations of foam films showed that the equilibrium film thickness in the presence of Jaguar is similar, $h_{EQ} \approx 100$ nm, which supports the explanation that Jaguar affects the foam properties by bridging the bubble surfaces.

It is known from the literature that the interactions between anionic surfactants and cationic polymers could be significantly affected by the presence of background electrolyte.[20,21] For this reason we performed additional experiments with BS + MAc + Jaguar solutions containing 150 mM NaCl. In these experiments, the Jaguar concentration was 0.01 wt %, because heavy sediments were observed at higher polymer concentrations. Figure 6A compares the total dimensionless stress vs capillary number for the BS + MAc + Jaguar mixtures at 0 and 150 mM NaCl. As mentioned above, in the BS + MAc + Jaguar system (no NaCl) we observe a maximum in the stress curve. However, no such maximum is seen in the presence of 150 mM NaCl; the total shear stress was the same as in the polymer-free foams.

For the systems obeying the Herschel–Bulkley law, see Figure 3A for results obtained with such systems, we determined the viscous stress by subtracting the yield stress from the total stress. Figure 6B presents the viscous stress vs capillary number for the BS and BS + Jaguar mixtures, with and without MAc, at 0 and 150 mM NaCl. We see that all data merge around two master lines, characteristic for the systems with MAc ($n \approx 0.25$) and without MAc ($n \approx 0.47$). Therefore, Jaguar and NaCl both do not affect the viscous stress for these systems, despite the fact that Jaguar strongly affects the yield stress for some of them.

From this series of experiments, we can conclude that the addition of Jaguar to the BS + LSM cousrfactant systems leads to increased yield stress of the foam. The addition of Jaguar to BS + HSM cosurfactant systems leads to a significant change in the shape of the total stress vs capillary number curve, which does not obey the Herschel–Bulkley law anymore. A higher concentration of Jaguar leads to higher stress at a given capillary number. When 150 mM NaCl is added to Jaguar-containing solutions, the rheological curves become similar to those of polymer-free foams. Under all conditions studied, no noticeable effect of Merquat was determined for the foam rheological properties.

4.4. Foam–Wall Friction. The results for the dimensionless wall stress, obtained with the BS and BS + MAc systems, containing Merquat of different concentrations, are compared in Figure S4 in the Supporting Information. One sees that the experimental data for all foams, stabilized with BS, merge around a master line with a power-law index $m \approx 2/3$, which indicates that the bubble surface in these mixtures is tangentially mobile. We should note that the dimensionless stress slightly decreases with increasing Merquat concentration in the foaming solutions (at the same value of the dimensionless velocity). This effect is not very pronounced

dx.doi.org/10.1021/la2035517 | Langmuir 2012, 28, 1115–1126

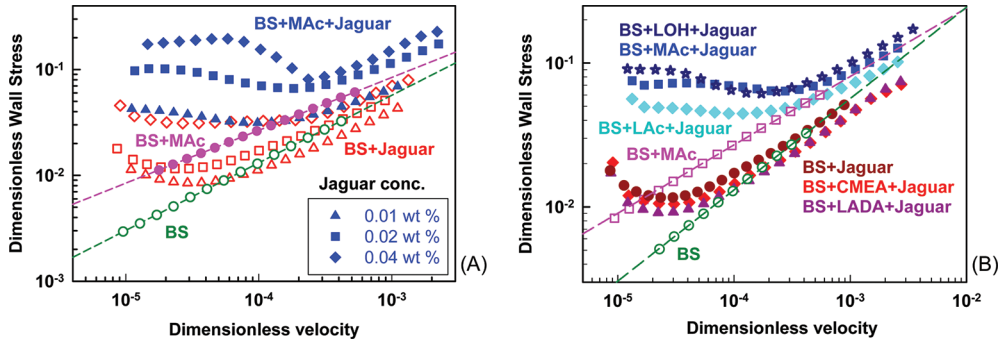

Figure 7. Dimensionless wall stress as a function of the dimensionless velocity for foams stabilized by (A) BS + Jaguar (red symbols) and BS + MAc + Jaguar (blue symbols) with different concentrations of Jaguar as indicated in the figure and (B) BS + 0.02 wt % Jaguar + 0.025 wt % different cosurfactants as indicated in the figure.

and could be partially due to insufficient accuracy in bubble size determination.

The data for the dimensionless wall stress in the experiments with BS + MAc merge around a master line with a power-law index $m \approx 1/2$, which indicates that the bubble surface is tangentially immobile in these systems. Therefore, the addition of Merquat to the surfactant mixtures BS and BS + MAc does not affect the regime of foam–wall friction for polymer concentrations up to 0.1 wt %.

In contrast, the addition of Jaguar leads to a significant change in the rheological curves for all systems studied; see Figure 7. For the systems containing LSM cosurfactants, the addition of Jaguar leads to a clear minimum in the stress vs rate rheological curve. For the systems containing HSM cosurfactant, the addition of polymer leads to the appearance of a wide range of shear rates in which the stress remains almost constant. Such a behavior suggests that the wetting films, formed between the bubbles and the solid wall, support an elastic stress connected to a strong adhesion between the bubble surface and the solid wall. The dimensionless wall stress increases with increasing Jaguar concentration for both LSM and HSM cosurfactants.

The appearance of a minimum in the rheological curve for LSM foams can be explained in the following way. The molecules of the cationic polymer form bridges between the surfaces of the bubbles and solid wall when the latter are not moving with respect to each other (see Figure 8). In this way,

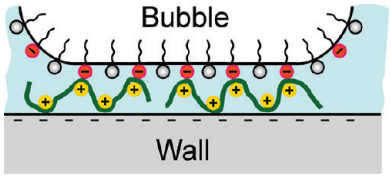

Figure 8. Schematic presentation of foam bubbles attached to a solid substrate by cationic polymer chains which bridge the surface of the wetting film.

the bubbles are attached to the wall surface. As the wall starts moving, an elastic component in the wall stress appears at low velocity, due to the stretching of the polymer chains. As the sliding progresses, a certain "wall yield stress" is exceeded, and the bubbles are detached from the wall surface. The measured stress is now due to the foam–wall viscous friction only, and the plot merges with that of the polymer-free system. Such wall yield stress has not been observed in the polymer-free systems.

The effect of NaCl on the foam–wall friction in Jaguar-containing foams was also studied. The obtained results are shown in Figure 9. One sees that NaCl suppresses the

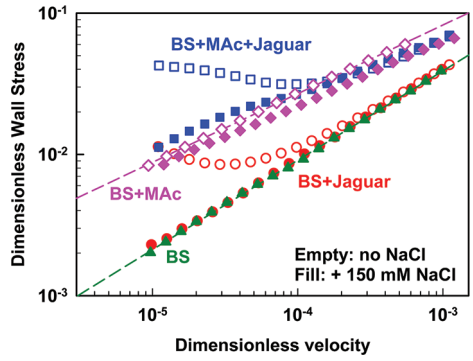

Figure 9. Dimensionless wall stress as a function of the dimensionless velocity for the foam–wall friction of foams stabilized by BS (green triangles), BS + MAc (pink tilted squares), BS + Jaguar (red circles), and BS + MAc + Jaguar (blue squares). The empty symbols indicate foams formed from solutions prepared with deionized water, whereas the full symbols are for foams containing 150 mM NaCl. The BS concentration is 0.5 wt %, the MAc concentration is 0.025 wt %, and the Jaguar concentration is 0.01 wt %.

minimum for the LSM foams and the plateau for the HSM systems in the stress–rate curve, which were observed in the systems with Jaguar (in the absence of NaCl). The solutions conctaining both polymer and NaCl are described well by a power law, similarly to the Jaguar-free systems. In conclusion, as in the case of bulk foam rheology, the addition of 150 mM NaCl eliminates the effect of Jaguar on the foam–wall friction.

4.5. Optical Observations of Foam Films. To check the hypothesis that the observed difference between Jaguar (strongly affecting foam properties) and Merquat (not affecting foam rheological properties) is due to their different interactions with the surfactant adsorption layers on the surfaces of the foam films, we performed optical observations of films formed in a capillary cell.

First, we performed experiments with films stabilized by BS solution. The BS system is a mixture of two low-molecular-mass surfactants with concentration higher than the cmc. Hence, the films formed from BS solution thinned like a typical low-molecular-mass surfactant system; see Figure 10 (first row). In the initial stage of film thinning, a dimple (thicker region in the film center) was formed and quickly ejected from the film. Then the film thickness decreased gradually to around 70 nm,

dx.doi.org/10.1021/la2035517 | Langmuir 2012, 28, 1115–1126

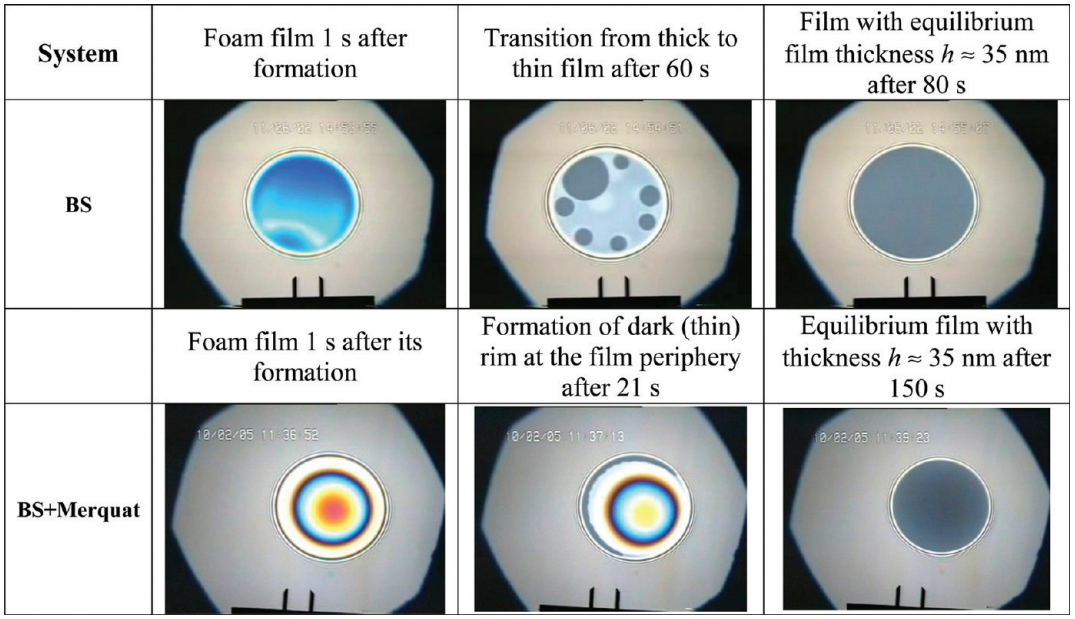

Figure 10. Images showing consecutive stages of the film-thinning process for the BS system (polymer-free solution, first row) and BS + Merquat system (second row). The distance between the two vertical dark bars is 50 μm.

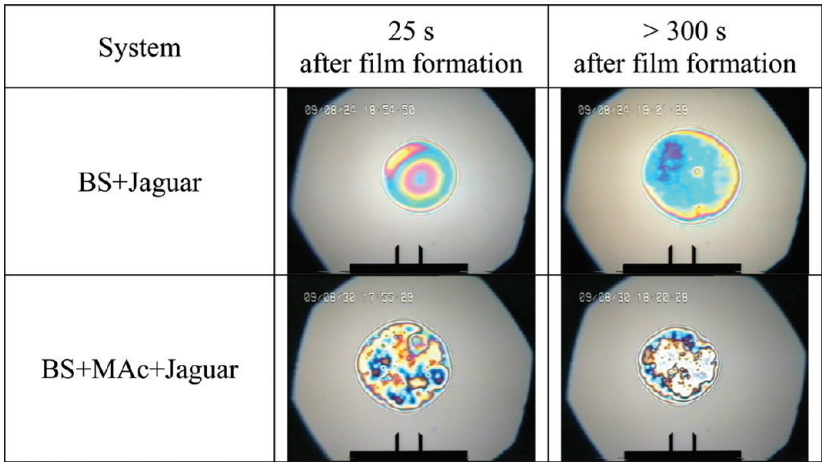

Figure 11. Consecutive images taken 25 and >300 s after film formation from solutions of 0.5 wt % BS + 0.02 wt % Jaguar (first row) and 0.5 wt % BS + 0.025 wt % MAc + 0.02 wt % Jaguar (second row). The distance between the two vertical bars is 50 μm.

where darker (thinner) spots were observed to form and expand until occupying the entire film area. Eventually, the film acquired its equilibrium thickness of $h \approx 35$ nm, which corresponds to the so-called "common black film", stabilized by electrostatic repulsion between the charged film surfaces.[32]

The thinning of the films formed from BS + Merquat solutions was slower and followed a slightly different evolution pattern. Instead of fast expelling of the dimple from the film into the surrounding meniscus region, the dimple was trapped in the film center and a thinner rim was formed at the film periphery; see Figure 10. Also, the stepwise transition was usually missing in these films, and a direct transition toward the final equilibrium film was observed. The final film thickness was almost the same for BS and BS + Meqruat solutions. These observations indicate that Merquat adsorbs on the film surfaces (otherwise it could not affect the film-thinning pattern), but the final equilibrium film is stabilized exclusively by the surfactant molecules.

The experiments with films formed from BS + MAc solutions showed that Merquat has no significant effect on this system. The thinning of the dimple is much slower than the thinning in the case of films from BS solution, which is due to the presence of MAc, which rigidifies the film surfaces.[8] The equilibrium film thickness is again ~35 nm. From all these experiments we can conclude that Merquat only slightly affects the thinning pattern of the films formed from the studied solutions, and the equilibrium film thickness is not affected by this polymer. These observations are in good agreement with the results from the rheological measurements.

Rather different results were obtained with Jaguar. All films formed from Jaguar-containing systems had very uneven thickness, due to the presence of polymer−surfactant aggregates, trapped between the film surfaces; see Figure 11 for illustrative images. The equilibrium film thickness was around 100 nm, which is in good agreement with the estimated thickness from the rheological data, at which the polymer has a significant impact on the foam rheological properties (70 nm).

dx.doi.org/10.1021/la2035517 | *Langmuir* 2012, 28, 1115−1126

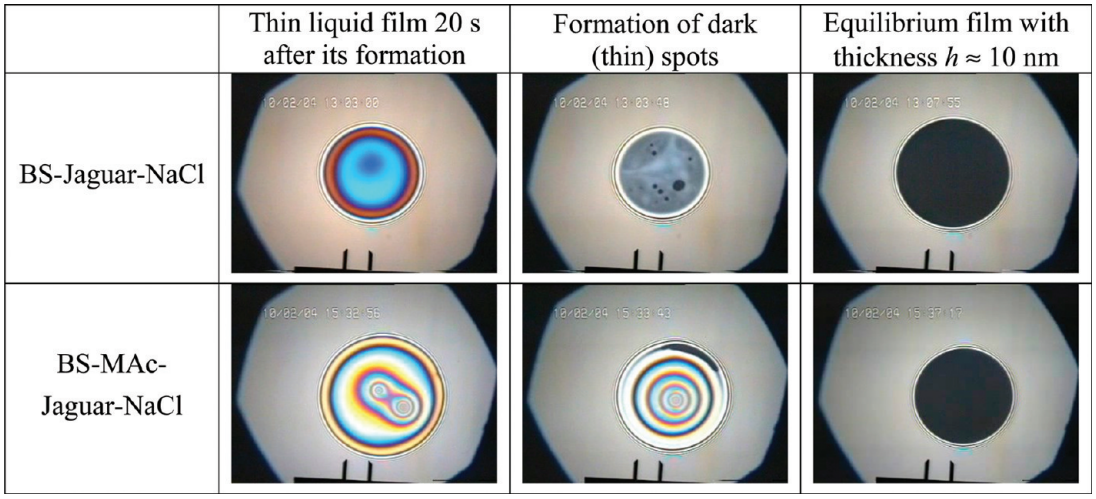

Figure 12. Images showing consecutive stages of film thinning for BS + Jaguar (first row) and BS + MAc + Jaguar (second row) solutions in the presence of 150 mM NaCl. The distance between the two vertical dark bars is 50 μm.

At the end of the film-thinning observations, we injected solution back into the capillary cell to separate the two opposite film surfaces from each other. Extra pressure was needed to separate the surfaces in the presence of Jaguar, and a large contact angle film meniscus was formed. This is clear evidence that Jaguar induces strong adhesion between the two opposite film surfaces for all systems studied. However, our current experimental setup does not allow quantitative measurement of this extra pressure, which would be a method to quantify the adhesion of the film surfaces.

We can conclude from these experiments that Jaguar significantly affects the thinning behavior of foam films in all BS + cosurfactant solutions. For both groups of cosurfactants (LSM and HSM) we observed Jaguar entrapment in the foam films, which explains why this polymer has a significant effect on the yield stress of sheared foams; see Figure 3. The effect is mainly due to the presence of trapped polymer molecules in the film area, which on its own leads to much stronger adhesion between the bubble surfaces.

As shown in the previous sections, the addition of NaCl to Jaguar-containing foams leads to the disappearance of the effect of Jaguar on the rheological curves. This result was explained with disappearance of the polymer bridges between the bubble surfaces. To check the latter hypothesis, we performed experiments in a capillary cell with films formed from BS + Jaguar and BS + MAc + Jaguar solutions containing 150 mM NaCl. Typical images from the respective foam films are shown in Figure 12. One sees that the presence of polymer is visible only in the first stage of film thinning, where some polymer−surfactant aggregates are seen inside the film. However, these aggregates leave the film area, and the subsequent pattern of film thinning is very similar to that observed in polymer-free systems. Therefore, we can conclude that Jaguar does not strongly adsorb on the bubble surface and does not affect the rheological properties of the foams in the presence of 150 mM NaCl. Most probably, the increased electrolyte concentration in the solution changes the interactions of the polymer with the surfactant molecules in a way that suppresses the polymer adsorption.

5. MAIN RESULTS AND CONCLUSIONS

We studied systematically the effect of two cationic surfactants (Merquat and Jaguar) on the rheological properties of foams, stabilized with a mixture of SLES + CAPB, in the presence of various cosurfactants which form an adsorption layer with high and low surface moduli. The obtained results can be summarized as follows.

The addition of Jaguar in the foaming solutions leads to (1) a significant increase of the foam yield stress for all systems studied (between 2- and 4-fold), (2) the presence of consecutive maximum and minimum in the $\tilde{\tau}$ vs Ca rheological curve for foams stabilized with cosurfactants having a high surface modulus (these systems cannot be described by the Herschel−Bulkley law anymore), and (3) the presence of significant foam−wall yield stress for all studied foams.

These effects are explained with the formation of polymer bridges between the bubbles and the wall (for foam−wall friction) and between the neighboring bubbles in slowly sheared foams (for inside foam friction). This explanation is supported by foam film observations, which show a very good correlation between the presence of polymer in the foam films and the polymer effect on the rheological properties of the foams.

Addition of 150 mM NaCl to Jaguar-containing systems eliminates the specific effects of Jaguar on foam rheology: the foams containing both Jaguar and NaCl behave similarly to the polymer-free systems. This result is also in good agreement with the foam film observations, which show that in the presence of 150 mM NaCl no Jaguar molecules are trapped in the foam films.

The addition of Merquat does not noticeably affect any of the rheological properties of the foams studied. The foam film observations and surface tension measurements showed that this polymer adsorbs weakly on the bubble surface and does not bridge the foam film surfaces.

These results demonstrate that the bubble−bubble attraction can be used for efficient control of the foam yield stress (and the foam−wall yield stress) without significantly affecting the viscous friction in sheared foams.

dx.doi.org/10.1021/la2035517 | *Langmuir* 2012, 28, 1115−1126

■ ASSOCIATED CONTENT

Supporting Information

Schematic presentation of the experimental setup used for rheological measurements, measured mean volume surface radius, R_{32}, as a function of the polymer concentration for the studied foams, measurements of the foam shear stress at different gap widths (varied between 1.5 and 3 mm) for the system BS + MAc + Jaguar, and measured dimensionless wall stress as a function of the dimensionless velocity for foam−wall friction of foams formed from solutions with different concentrations of Merquat. This material is available free of charge via the Internet at http://pubs.acs.org.

■ AUTHOR INFORMATION

Corresponding Author

*Phone: (+359-2) 962 5310. Fax: (+359-2) 962 5643. E-mail: SC@LCPE.UNI-SOFIA.BG.

■ ACKNOWLEDGMENTS

We are grateful to Mrs. Radka Petkova for performing the experiments with foam films and to Mrs. Mila Temelska for the measurements of the surface modulus (both from the Sofia University). The study is funded by the Unilever R&D Center in Trumbull, CT, and by the National Science Fund of Bulgaria (Program Rila-4).

■ REFERENCES

(1) Princen, H. M. The structure, mechanics, and rheology of concentrated emulsions and fluid foams. In *Encyclopedia of Emulsion Technology*; Sjöblom, J., Ed.; Marcel Dekker: New York, 2001; Chapter 11, p 243.

(2) Weaire, D. The rheology of foam. *Curr. Opin. Colloid Interface Sci.* **2008**, *13*, 171.

(3) Kraynik, A. M. Foam flows. *Annu. Rev. Fluid Mech* **1988**, *20*, 325.

(4) Princen, H. M. Rheology of foams and highly concentrated emulsions: I. Elastic properties and yield stress of a cylindrical model system. *J. Colloid Interface Sci.* **1983**, *91*, 160.

(5) Princen, H. M. Rheology of foams and highly concentrated emulsions. II. Experimental study of the yield stress and wall effects for concentrated oil-in-water emulsions. *J. Colloid Interface Sci.* **1985**, *105*, 150.

(6) Princen, H. M.; Kiss, A. D. Rheology of foams and highly concentrated emulsions: IV. An experimental study of the shear viscosity and yield stress of concentrated emulsions. *J. Colloid Interface Sci.* **1989**, *128*, 176.

(7) Denkov, N. D.; Subraminian, V.; Gurovich, D.; Lips, A. Wall slip and viscous dissipation in sheared foams: Effect of surface mobility. *Colloids Surf., A* **2005**, *263*, 129.

(8) Golemanov, K.; Denkov, N. D.; Tcholakova, S.; Vethamuthu, M.; Lips, A. Surfactant mixtures for control of bubble surface mobility in foam studies. *Langmuir* **2008**, *24*, 9956.

(9) Denkov, N. D.; Tcholakova, S.; Golemanov, K.; Ananthapadmanabhan, K. P.; Lips, A. Viscous friction in foams and concentrated emulsions under steady shear. *Phys. Rev. Lett.* **2008**, *100*, 138301.

(10) Tcholakova, S.; Denkov, N. D.; Golemanov, K.; Ananthapadmanabhan, K. P.; Lips, A. Theoretical model of viscous friction inside steadily sheared foams and concentrated emulsions. *Phys. Rev. E* **2008**, *78*, 011405.

(11) Rouyer, F.; Cohen-Addad, S.; Vignes-Adler, M.; Hoehler, R. Dynamics of yielding observed in a three-dimensional aqueous dry foam. *Phys. Rev. E* **2003**, *67*, 021405.

(12) Marze, S.; Langevin, D.; Saint-Jalmes, A. Aqueous foam slip and shear regimes determined by rheometry and multiple light scattering. *J. Rheol.* **2008**, *52*, 1091.

(13) Denkov, N. D.; Tcholakova, S.; Golemanov, K.; Lips, A. Jamming in sheared foams and emulsions, explained by critical instability of the films between neighboring bubbles and drops. *Phys. Rev. Lett.* **2009**, *103*, 118302.

(14) Golemanov, K.; Tcholakova, S.; Denkov, N. D.; Ananthapadmanabhan, K. P.; Lips, A. Breakup of bubbles and drops in steadily sheared foams and concentrated emulsions. *Phys. Rev. E* **2008**, *78*, 051405.

(15) Denkov, N.; Tcholakova, S.; Golemanov, K.; Ananthapadmanabhan, K. P.; Lips, A. Role of surfactant type and bubble surface mobility in foam rheology. *Soft Matter* **2009**, *7*, 3389.

(16) Durand, M.; Stone, H. A. Relaxation time of the topological T1 process in a two-dimensional foam. *Phys. Rev. Lett.* **2006**, *97*, 226101.

(17) Soller, R.; Koehler, S. A. Rheology of steady-state draining foams. *Phys. Rev. Lett.* **2008**, *100*, 208301.

(18) Larmignat, S.; Vanderpool, D.; Lai, H. K.; Pilon, L. Rheology of colloidal gas aphrons (microfoams). *Colloid Surf., A* **2008**, *322*, 199.

(19) Zhao, J.; Pillai, S.; Pilon, L. Rheology of microfoams made from ionic and non-ionic surfactant solutions. *Colloid Surf., A* **2009**, *348*, 93.

(20) Goddard, E. D. Polymer-surfactant interaction. Part II. Polymer and surfactant of opposite charge. *Colloids Surf., A* **1986**, *19*, 301.

(21) Goddard, E. D.; Hannan, R. B. Cationic polymer/anionic surfactant interactions. *J. Colloid Interface Sci.* **1976**, *55*, 73.

(22) Bergeron, V.; Langevin, D.; Asnacios, A. Thin-film forces in foam films containing anionic polyelectrolyte and charged surfactants. *Langmuir* **1996**, *12*, 1550.

(23) Kleinschmidt, F.; Stubenrauch, C.; Delacotte, J.; von Klitzing, R.; Langevin, D. Stratification of foam films containing polyelectrolytes. Influence of the polymer backbone's rigidity. *J. Phys. Chem. B* **2009**, *113*, 3972.

(24) Qu, D.; Brotons, G.; Bosio, V.; Fery, A.; Salditt, T.; Langevin, D.; von Klitzing, R. Interactions across liquid thin films. *Colloids Surf., A* **2007**, *303*, 97.

(25) Garrett, P. R.; Hines, J. D.; Joyce, S. C.; Whittal, P. T. Report prepared for Unilever R&D, Port Sunlight, U.K., 1993.

(26) Mukherjee, S.; Wiedersich, H. Morphological and viscoelastic properties of dense foams generated from skin cleansing bars. *Colloids Surf.* **1995**, *95*, 159.

(27) Scheludko, A. Thin liquid films. *Adv. Colloid Interface Sci.* **1967**, *1*, 391.

(28) Mason, T. G.; Bibette, J.; Weitz, D. A. Yielding and flow of monodisperse emulsions. *J. Colloid Interface Sci.* **1996**, *179*, 439.

(29) Mason, T. G. Rheology of monodisperse emulsions. Ph.D. Thesis, Department of Physics, Princeton University, Princeton, NJ, 1995.

(30) Seth, J. R.; Mohan, L.; Locatelli-Champagne, C.; Cloitre, M.; Bonnesaze, R. A micromechanical model to predict the flow of soft particle glasses. *Nat. Mater.* **2011**, *10*, 838.

(31) Sexton, M. B.; Möbius, M. E. M.; Hutzler, S. Bubble dynamics and rheology in sheared two-dimensional foams. *Soft Matter* **2011**, *7*, 11252.

(32) Kralchevsky, P. A.; Danov, K. D.; Denkov, N. D. In *Handbook of Surface and Colloid Chemistry*; Birdi, K. S., Ed.; CRC Press LLS: Boca Raton, FL, 1997; Chapter 11.